Biochimica et Biophysica Acta 1807 (2011) 813–818

Contents lists available at ScienceDirect

Biochimica et Biophysica Acta

journal homepage: www.elsevier.com/locate/bbabio

Stabilization of the peroxy intermediate in the oxygen splitting reaction of cytochrome cbb_3 ☆

Vivek Sharma [a,*], Mårten Wikström [a,*], Ville R.I. Kaila [a,b,c,*]

[a] Helsinki Bioenergetics Group, Programme for Structural Biology and Biophysics, Institute of Biotechnology, PB 65 (Viikinkaari 1), University of Helsinki, 00014, Finland
[b] Department of Chemistry, PB 55 (A. I. Virtanens plats 1), University of Helsinki 00014, Finland
[c] Laboratory of Chemical Physics, National Institute of Diabetes and Digestive and Kidney Diseases, National Institutes of Health, Bethesda, MD 20892-0520, USA

ARTICLE INFO

Article history:
Received 1 December 2010
Received in revised form 2 February 2011
Accepted 4 February 2011
Available online 20 February 2011

Keywords:
Density Functional Theory (DFT)
cbb_3-type cytochrome *c* oxidase
Oxygen activation
Oxygen affinity
Heme-copper oxidases

ABSTRACT

The proton-pumping cbb_3-type cytochrome *c* oxidases catalyze cell respiration in many pathogenic bacteria. For reasons not yet understood, the apparent dioxygen (O_2) affinity in these enzymes is very high relative to other members of the heme-copper oxidase (HCO) superfamily. Based on density functional theory (DFT) calculations on intermediates of the oxygen scission reaction in active-site models of cbb_3- and aa_3-type oxidases, we find that a transient peroxy intermediate (**I_P**, Fe[III]–OOH^-) is ~6 kcal/mol more stable in the former case, resulting in more efficient kinetic trapping of dioxygen and hence in a higher apparent oxygen affinity. The major molecular basis for this stabilization is a glutamate residue, polarizing the proximal histidine ligand of heme b_3 in the active site.

Published by Elsevier B.V.

1. Introduction

Heme-copper oxidases (HCO) are transmembrane respiratory enzymes responsible for reducing molecular oxygen to water with electrons and protons taken from opposite sides of the mitochondrial or bacterial membrane [1–3]. The electric "charging" of the membrane is further amplified when energy released from the oxygen reduction is used for concomitant proton-pumping across the membrane [1–3]. The substrate oxygen enters the active site of the enzyme through an oxygen diffusion channel, whilst electrons traverse to the active-site through the metal centers. Protons are transferred by the assistance of polar amino acid side-chains and water molecules, and are directed both to the active-site and across the membrane [4–6] as a result of the electron transfer reactions [7–9].

Based on various classification methods, the HCO enzymes can be divided into at least three subfamilies, A, B, and C [10–13]. The best studied subclass of the HCO superfamily is the A-class or the aa_3-type oxidases [5,6], the reaction cycle of which begins by binding dioxygen to the reduced ferrous-cuprous heme a_3/Cu_B active site, producing the **A-**state [1,14]. In the absence of electrons in Cu_A or heme *a*, this leads to scission of the O-O bond in ~200 μs, where out of the total of four electrons required, two are supplied by the high-spin heme, one by Cu_B and the fourth most probably by a tyrosine residue cross-linked to one of the histidine ligands of the copper [15]. The resulting **P_M** state is characterized by a ferryl heme (Fe[IV] O^{2-}), a cupric copper with a hydroxyl ligand (Cu_B[II]—OH^-), and a neutral tyrosine radical (Tyr—O^*). Electron transfer from the nearby heme leads to reduction of the tyrosine radical to a tyrosinate (Tyr—O^-), the **P_R** state [16], which is the state formed directly from state **A** when the fully reduced enzyme reacts with dioxygen. The **P_M** and **P_R** states are analogous to the well-studied Compounds I (Fe[IV] O^{2-} and a cation radical) and II (Fe[IV] O^{2-}) of many heme enzymes [17].

The distant cbb_3- or C-type members of the HCO superfamily have been much less studied [12,13], but the crystal structure of one member of this subfamily was recently solved [18]. The cbb_3 enzymes are found in many bacteria, including the pathogens *Helicobacter* and *Campylobacter*, that live under micro-aerobic conditions and show a very high apparent affinity for oxygen (K_M ~7 nM) relative to their A-class counterparts (K_M ~0.1–1 μM) [19]. C-type oxidases also show deviant ligand (CO, NO and O_2) binding properties as compared to the A-type oxidases [19,20]. For example, CO has been suggested to bind more linearly to the heme b_3 with faster recombination kinetics after photolysis [20,21]. Biochemical and biophysical experiments done prior to the recently available crystal structure suggested two important functional motifs in the cbb_3 enzymes; a) presence of a cross-linked tyrosine analogous to that in the A-type enzymes, but originating from a different transmembrane helix and, b) the unique presence of a proximal glutamic acid residue hydrogen-bonded to the

Abbreviations: HCO, heme-copper oxidase; DFT, density functional theory; BNC, binuclear center

☆ Amino acid numbers corresponding to aa_3-type oxidase from *Paracoccus denitrificans* and cbb_3-type oxidase from *Rhodobacter sphaeroides* are denoted with A: and C: prefixes, respectively.

* Corresponding authors. Tel.: +358 9 191 59751; fax: +358 9 191 59920.
E-mail addresses: vivek.sharma@helsinki.fi (V. Sharma), marten.wikstrom@helsinki.fi (M. Wikström), ville.kaila@nih.gov (V.R.I. Kaila).

0005-2728/$ – see front matter. Published by Elsevier B.V.
doi:10.1016/j.bbabio.2011.02.002

histidine ligand of heme b_3 [22–26]. Homology modeling studies and density functional theory (DFT) calculations on small model systems further suggested that these structural differences in the active-site of C-type oxidases could result in different ligand binding characteristics [12,27,28]. As previously suggested [12,24], the crystal structure shows that the C-type oxidases comprise only one proton conduction channel [18] at the location of the "canonical" K-channel [29], and similar to what has also been observed for the B-class HCOs [30].

Verkhovsky et al. [31] showed that the early kinetics of the reaction of A-type cytochrome *c* oxidase with O_2 required postulation of an intermediate (called P/S, for peroxy/superoxy) between the oxy state **A** and the $\mathbf{P_R}$ state (then called P1). The energy of the P/S intermediate was estimated to be a few kcal/mol above state **A**. Computational approaches have been successfully used on the active-site models of A-type oxidases to address questions related to the energetics of the reaction or of the proton-pumping mechanism [32–43]. DFT studies by Blomberg et al. [44–46] on the active-site models of A-type oxidase suggested the presence of a similar ferric peroxy intermediate (called $\mathbf{I_P}$), which was proposed to lie a few kcal/mol higher in energy relative to the **A** state. Recent quantum chemical modeling of this initial oxygen reduction reaction by Yoshioka et al. [36] further implied that a water molecule assists the proton transfer from the cross-linked tyrosine to the heme-bound oxygen, which will result in formation of the ferric-peroxy intermediate. Similar DFT calculations have been performed on the models of the B-type oxidase from *Thermus thermophilus* [47].

Assuming that the oxygen splitting reaction proceeds via a similar peroxy-intermediate in cbb_3-type oxidases, we have compared the $\mathbf{A} \rightarrow \mathbf{I_P} \rightarrow \mathbf{P_M}$ reaction sequence in aa_3- and cbb_3-type oxidases using quantum chemical DFT calculations. The calculations suggest that the $\mathbf{I_P}$ intermediate is more stable in the cbb_3 oxidases than in the aa_3 enzymes, providing a molecular explanation for the higher apparent dioxygen affinity of the former.

2. Models and methods

Model systems representing aa_3- and cbb_3-type oxidases ($\mathbf{A_L}$/$\mathbf{C_L}$) by ~200 atoms were constructed from the crystal structure of CcO from *Paracoccus denitrificans* (PDB ID: 1QLE) [48] and homology models of cbb_3-type oxidase from *Rhodobacter sphaeroides*, [12,27] respectively, consisting of the high-spin heme (a_3/b_3), its histidine ligand (A:H411, C:H405☆). propionate groups and their immediate hydrogen bonding partners (A:W164/C:Y181 and A:R473/C:R471 and, A:H403/C:H397 and A:D399/C:N393), Cu_B, and its histidine ligands (A:H325/C:H317, A:H326/C:H318 and A:H276/C:H267) and cross-linked tyrosine (A:Y280/C:Y311). The histidines A:H403/C:H397 were methylated at Nε2 positions to avoid transfer of the Nδ1 proton to the respective A-propionate (Figure S1, Supplementary Information). The hydrogen bonding partner of the proximal histidine ligand (C:H405), glutamic acid (C:E383) was also modeled based on recent studies [22], as described in Ref. [28]. A water molecule, rationalizing the proton transfer from the cross-linked tyrosine to the dioxygen was also modeled (Fig. 1a and d), in analogy to the studies on A-type oxidases [36,38,44–46].

During finalization of this work, the crystal structure of the cbb_3-oxidase from *Pseudomonas stutzeri* was published (PDB ID: 3MK7) [18]. We observe that our active-site models closely resemble the crystal structure, including the cross-linked tyrosine conformation as well as the presence of hydrogen bonding glutamic acid in the proximal cavity. However, the modeled heme propionate–protein interactions were incorrect. Instead of the modeled arginine (C:R471), a Ca^{2+} ion neutralizes the negative charge of the D-propionate of the high-spin heme in the crystal structure [18]. To study the sensitivity of this interaction on the energies, we constructed smaller test systems from the optimized geometries of larger systems for both enzymes, without including the propionates or their interaction partners.

Three different intermediate states of the oxygen reduction reaction ($\mathbf{A} \rightarrow \mathbf{I_P} \rightarrow \mathbf{P_M}$, Fig. 2a) were studied in both enzyme model systems, aa_3

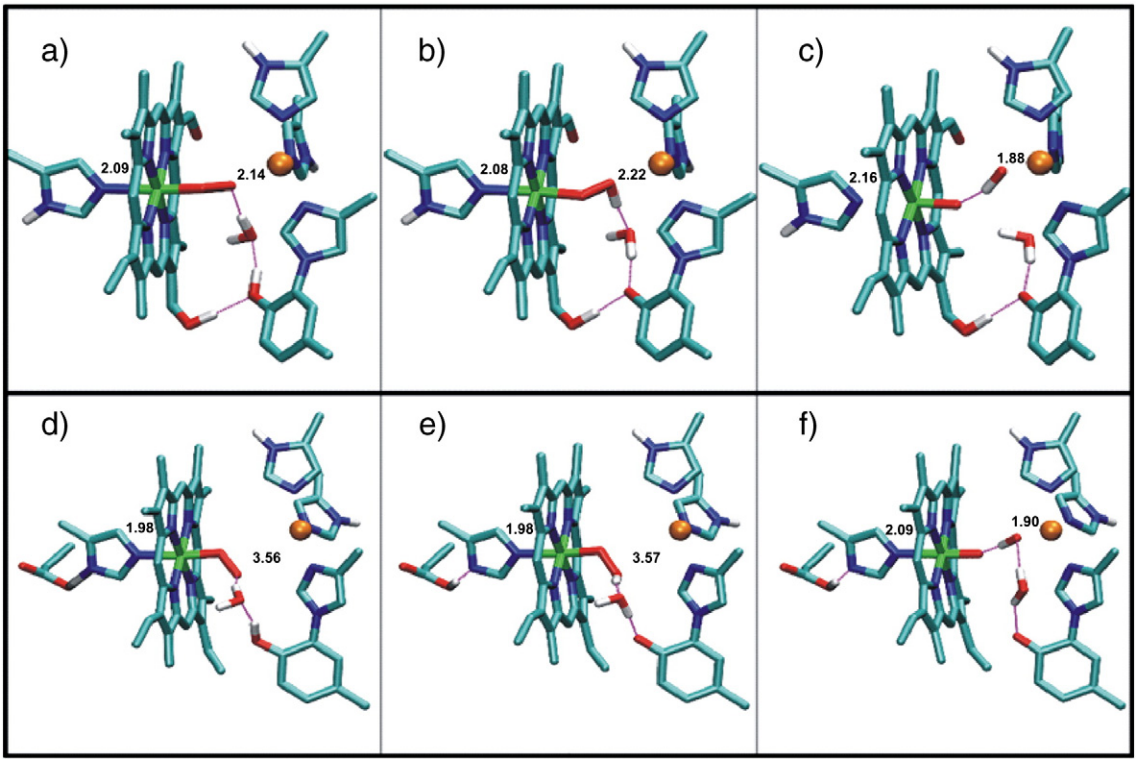

Fig. 1. DFT optimized structures of **A** (a, d), $\mathbf{I_P}$ (b, e) and $\mathbf{P_M}$ (c, f) intermediates in aa_3- (top, $\mathbf{A_L}$) and cbb_3-type oxidases (bottom, $\mathbf{C_L}$). Carbon (cyan), oxygen (red), nitrogen (blue), iron (green) and copper (orange) are shown. Only hydrogen atoms connected to nitrogen and oxygen atoms are shown. Propionate interactions are omitted for clarity and distances Fe—$N\epsilon_{His}$, and Cu_B—O^d are reported in Angstroms. Hydrogen bonds are shown with purple dotted lines. The figure was prepared using VMD [57].

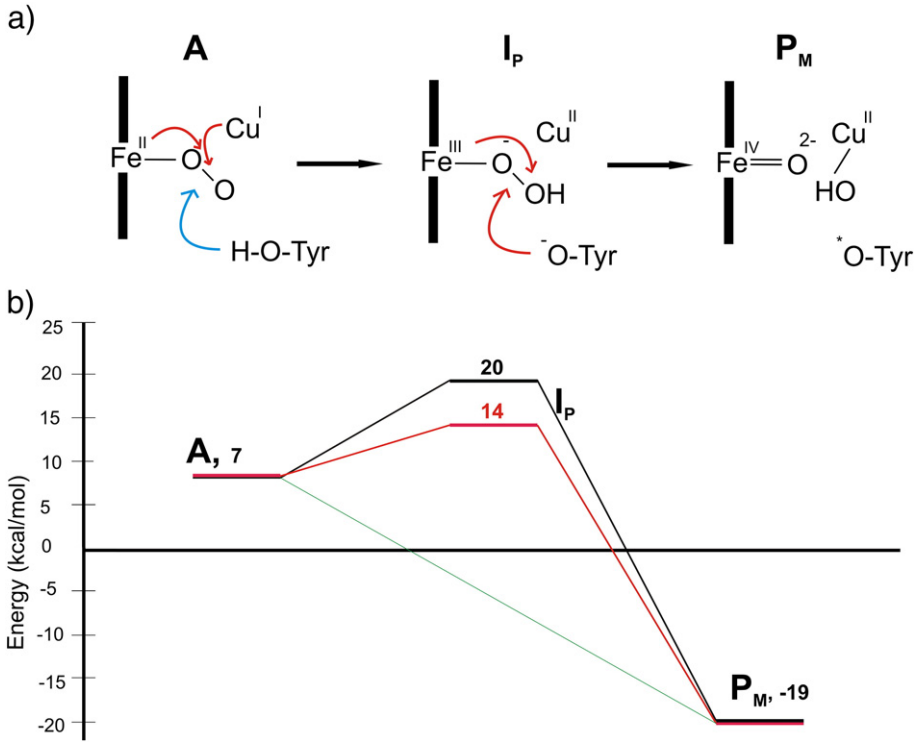

Fig. 2. a) Modeled reaction sequence from **A**→**I**$_P$→**P**$_M$ is shown. Red and blue arrows show proposed electron and proton transfer paths. b) Electronic energies (in kcal/mol) of the reaction sequence for two enzyme model systems (red—**C**$_L$ and black—**A**$_L$) are shown. The energies of states **I**$_P$ and **P**$_M$ are relative to state **A**.

(**A**$_L$) and *cbb*$_3$ (**C**$_L$) type; i) **A** (Fe[II]-O_2/Cu[I]/Tyr-OH), ii) **I**$_P$ (Fe[III]—OOH^-/Cu[II]/Tyr—O^-) and iii) **P**$_M$ (Fe[IV] O^{2-}/Cu[II]—OH^-/Tyr—O^*), named here as **A**$_L$**-A**/**C**$_L$**-A**, **A**$_L$**-I**$_P$/**C**$_L$**-I**$_P$, and **A**$_L$**-P**$_M$/**C**$_L$**-P**$_M$, respectively. In the modeled reaction the proton is transferred from the cross-linked Tyr to the oxygenous species in the **I**$_P$-state as shown in Fig. 2a and via the bridging water molecule (Fig. 1a and d). Charge and spin of each state are shown in Table 1.

Amino acid side-chains were cut at the C_β positions, which were kept frozen during the structure optimization at the BP86 [49,50] level of theory using a split valence polarized (def2-SVP) basis set for all atoms except the metals, which were defined with a triple-zeta valence polarized (def2-TZVP) basis set [51,52]. The RI approximation was used during the geometry optimization [53]. Figure S1 shows the complete structure of both enzyme model systems (**A**$_L$**-A** and **C**$_L$**-A**) with fixed atoms highlighted. Energy differences relative to the **A** state were calculated at the B3LYP [49,54] level with a TZVP basis set for all atoms, along with dielectric environment ($\epsilon = 4$) defined using the COSMO model [55]. Due to the high computational cost of evaluating the Hessian matrix (second derivative of energy with respect to coordinate displacement) for a large system comprising >200 atoms, optimization of the transition states that combine **A**, **I**$_P$ and **P**$_M$ was considered outside the scope of the present study.

All calculations were done with TURBOMOLE 5.10 and 6.1 [56] and Visual Molecular Dynamics (VMD) was used for visualization [57]. Default convergence criteria of TURBOMOLE was used in the calculations (energy gradient = 10^{-6} Hartree and geometry gradient = 10^{-3} a.u.).

The aim of this study is not to estimate the binding constant of the dioxygen in the two different enzymes, which is rather weak and subjected to possible DFT problems [58,59], but to explain the molecular basis of the strong apparent affinity (lower K_M) shown by one of the enzymes relative to the other.

Table 1
Spin (s), total charge (q) and total number of atoms (n) in the model systems studied.

Model	s	q	n
A$_L$**-A**	0	1	205
A$_L$**-I**$_P$	0	1	205
A$_L$**-P**$_M$	1	1	205
C$_L$**-A**	0	0	214
C$_L$**-I**$_P$	0	0	214
C$_L$**-P**$_M$	1	0	214

3. Results and discussion

3.1. Geometrical characteristics

Structural analysis of the two model systems representing the enzymes of *aa*$_3$ and *cbb*$_3$ type, (**A**$_L$ and **C**$_L$, respectively) in states **A**, **I**$_P$, and **P**$_M$, is presented in Table 2 and Fig. 1. The proton shared between the proximal histidine ligand and glutamate in the *cbb*$_3$-models is found closer to the latter residue in all studied states, suggesting a stronger stabilization of the ferric/ferryl heme iron relative to the *aa*$_3$-models, where no such glutamate residue exists. This is also

Table 2
Geometrical data of the model systems studied. All distances are in Å.

Model	Fe-Nϵ_{His}[a]	Nδ_{His}[a]-H[c]	Oϵ_{Glu}[b]-H[c]	Cu_B-O[d]	Fe-O[e]	O[d]-O[e]
A$_L$**-A**	2.09	1.02	–	2.14	1.77	1.33
A$_L$**-I**$_P$	2.08	1.02	–	2.22	1.81	1.47
A$_L$**-P**$_M$	2.16	1.02	–	1.88	1.65	2.71
C$_L$**-A**	1.98	1.53	1.07	3.56	1.78	1.31
C$_L$**-I**$_P$	1.98	1.55	1.06	3.57	1.80	1.40
C$_L$**-P**$_M$	2.09	1.56	1.06	1.90	1.66	2.75

[a] Proximal histidine (A:H411 or C:H405).
[b] Glutamic acid (C:E383).
[c] Proton shared between histidine and glutamic acid in *cbb*$_3$-models.
[d] Oxygen atom away from iron in **A** and **I**$_P$, and bound to Cu_B in **P**$_M$.
[e] Oxygen atom bound to (closer to) iron in **A**, **I**$_P$ and **P**$_M$.

supported by the shorter distance between the proximal histidine ligand and heme iron in the cbb_3-models, in accordance with our previous studies [28]. In both model systems the oxygen splitting is evident from the weakening of the O—O bond with the increase in O—O bond distance as the reaction proceeds. This correlates with an increase in the double bond character of the Fe—O bond during $\mathbf{I_P} \rightarrow \mathbf{P_M}$, in harmony with previous studies on the aa_3-system [44–46]. The different orientation of the cross-linked tyrosine in the cbb_3-model relative to the aa_3-model causes a stronger interaction between the tyrosine and the distal ligand of heme iron mediated via the bridging water molecule, as can be observed from the shorter distances between peroxy-ligand and the water molecule ($d(\mathbf{A_L}\text{-}\mathbf{I_P}) = 1.61$ Å, $d(\mathbf{C_L}\text{-}\mathbf{I_P}) = 1.51$ Å) as well as the tyrosine and the water ($d(\mathbf{A_L}\text{-}\mathbf{I_P}) = 1.63$ Å, $d(\mathbf{C_L}\text{-}\mathbf{I_P}) = 1.57$ Å).

3.2. Energetics of the oxygen splitting reaction

In the reaction sequence $\mathbf{A} \rightarrow \mathbf{I_P} \rightarrow \mathbf{P_M}$, the $\mathbf{I_P}$ intermediate is ~6 kcal/mol more stable in the cbb_3-model relative to the aa_3-model (Fig. 2b). Verkhovsky et al. [31] showed that the rate of the analogous formation of the $\mathbf{P_R}$ state could be described as $k[\mathbf{I_P}]$, where k is the rate constant and $[\mathbf{I_P}]$ is the occupancy of the peroxy intermediate. Hence, the observed stabilization of intermediate $\mathbf{I_P}$ in the cbb_3 enzyme would correspond to a four orders of magnitude higher rate of product formation. Such enhancement of the rate of kinetic oxygen trapping [60,61] would be expected to lower the apparent Michaelis constant, K_M, in the cbb_3-enzymes in harmony with experimental data [19]. The observed stabilization is not sensitive to the exact propionate interactions because a ~5 kcal/mol stabilization of the $\mathbf{I_P}$ state is also observed in the smaller test system of the aa_3-/cbb_3-oxidases (see section 2), suggesting that the propionate interactions are not critical for the initial reaction with oxygen.

Deducting a 10 kcal/mol loss in entropy [62] (increase in free energy) upon binding of a diatomic molecule, gives an overall exergonicity of ~10 kcal/mol for **R** (zero level in Fig. 2b) $\rightarrow \mathbf{P_M}$ for both enzymes, comparing well to previous estimates of the energetics in the aa_3-enzymes [44–46]. As has been previously pointed out [58,59], quantitative agreement with experiments for the oxygen binding and splitting reaction has not been obtained, indicating possible DFT problems in describing open-shell singlet states [62,63], dispersive interactions [64,65] and/or that the computational models of the binuclear center are missing essential parts. However, as the possible problem is present in both studied model systems, this is unlikely to affect the *relative* energetics of the $\mathbf{A} \rightarrow \mathbf{I_P}$ reaction in the two enzymes. The energy levels of **A** and $\mathbf{P_M}$ relative to state **R**, are nearly identical in both enzyme models, further supporting the notion that dioxygen is kinetically rather than thermodynamically trapped to the active site of heme-copper oxidases [31,60,61].

As a result of the stabilized $\mathbf{I_P}$ state in the cbb_3 oxidase models, there might be a possibility to observe this intermediate experimentally, by analogy to a peroxy-state observed in cytochrome *bd*, an enzyme with a high-affinity for dioxygen [66,67]. Aoyama et al. [68] and Koepke et al. [69] have independently suggested that a stable dianionic peroxide might reside within the fully oxidized active site of cytochrome aa_3. However, the crystallographically observed oxygenous species in these studies is more likely to have resulted from dioxygen, possibly in combination with X-ray radiation [70].

3.3. Electrostatics stabilization

Analysis of the electrostatic interactions between the distal ligand of heme iron and the surroundings, based on the Merz–Kollman charges [71] and the geometry, indicates that the $\mathbf{I_P}$ state is electrostatically stabilized by ~10 kcal/mol in the cbb_3 model relative to the aa_3-model (Table 3). The main difference in the cbb_3 system is obtained from a stabilization of the interaction between the ligand and the heme b_3/the proximal histidine, during the $\mathbf{A} \rightarrow \mathbf{I_P}$ transition (Tables 3 and 4), where the ligand is strongly polarized by the presence of the proximal glutamate (see below). This also agrees with the shorter Fe–Nε_{His} distance (Table 2 and Fig. 1) and a higher oxidized character of the iron in the cbb_3-model system, as discussed above and predicted in our earlier study [28]. Interestingly, the distal iron ligand (O_2, OOH^- or O^{2-}) has a more negative charge in all states in the cbb_3-models relative to aa_3 (Table 4).

Table 3
Differences in electrostatic interaction energies (in kcal/mol) between the oxygenous ligand and the group reported in the table. The interaction energies are computed from optimized geometries and Merz–Kollman charges during $\mathbf{A} \rightarrow \mathbf{I_P}$ transition in aa_3 and cbb_3 models.

Group	E_{aa3}[a]	E_{cbb3}[a]	$\Delta E_{(cbb3\text{-}aa3)}$
Cu_B	+6.1	+12.0	+5.9
[b]His	+8.7	+3.2	−5.5
[c]heme	+4.6	−1.9	−6.5
[d]WT	−19.5	−10.1	+9.4
[e]His	−0.2	−11.5	−11.3
[f]Tyr:	+2.9	+2.7	−0.2
[g]Glu	–	−1.3	−1.3
others	+12.2	+12.8	+0.6
V_{tot}	+14.8	+4.8	−10

[a] Electrostatic interaction energy difference ($\mathbf{I_P}$-**A**).
[b] Histidine ligands of Cu_B (sum of charges).
[c] High spin heme *a* or *b* type.
[d] Bridging water molecule.
[e] Proximal histidine (A:H411 or C:H405).
[f] Cross-linked tyrosine (A:Y280 or C:Y311).
[g] Glutamic acid (C:E383).

The presence of glutamate in hydrogen bonding distance with the proximal histidine ligand is a unique structural feature among the HCO superfamily, known only in the cbb_3-type oxidases, whilst this motif is present in e.g. cytochrome c peroxidase [72]. This interaction is found to stabilize the peroxy ($\mathbf{I_P}$) intermediate in the oxygen scission reaction; the glutamate acts as a proton acceptor for the proximal histidine and causes redistribution of the charges of heme b_3. Partial deprotonation of the histidine leads to an increased imidazolate character, electronically analogous to the negatively charged thiolate heme ligand found in the cytochrome P450 family. The thiolate has been suggested to act by a "push" effect [73,74], with crucial importance in the O—O bond cleavage and formation of Compound I. Olgiaro et al. [75] analyzed the effect by quantum chemical calculations and found that classical electrostatic field effects were dominating in the postulated mechanism. The electrostatic effects found in the cbb_3 oxidases suggest that the glutamate-histidine ligand might act by a similar "push" effect to gain rate acceleration relative to the aa_3 oxidases. The interaction between the histidine and glutamate in cytochrome *c* peroxidases has been subjected to many previous studies [72,76,77], supporting the strong electrostatic effect. It has been suggested based on hybrid quantum mechanics/molecular

Table 4
Merz–Kollman charges obtained at B3LYP/TZVP/$\epsilon = 4$ level.

Model	Fe	heme[a]	Cu_B	His[b]	Lig[c]	His[d]	Glu[e]	Tyr[f]	WT[g]
$\mathbf{A_L}$-**A**	2.10	−3.24	0.28	0.16	−0.46	0.57	–	0.01	−0.07
$\mathbf{A_L}$-$\mathbf{I_P}$	1.94	−3.01	0.38	0.21	−0.18	0.55	–	−0.42	−0.10
$\mathbf{A_L}$-$\mathbf{P_M}$	1.99	−3.07	0.62	0.15	−0.68	0.75	–	0.17	−0.01
$\mathbf{C_L}$-**A**	2.40	−3.26	0.38	−0.53	−0.60	0.49	−0.17	−0.09	−0.03
$\mathbf{C_L}$-$\mathbf{I_P}$	2.02	−2.70	0.33	−0.40	−0.26	0.57	−0.16	−0.76	−0.07
$\mathbf{C_L}$-$\mathbf{P_M}$	1.83	−2.59	0.66	−0.55	−0.85	0.74	−0.15	0.02	−0.06

[a] High spin heme *a* or *b* type.
[b] Proximal histidine (A:H411 or C:H405).
[c] heme iron ligand (O_2, OOH^- or O^{2-}).
[d] Histidine ligands of Cu_B (sum of charges).
[e] Glutamic acid (C:E383).
[f] Cross-linked tyrosine (A:Y280 or C:Y311).
[g] Bridging water molecule.

mechanics (QM/MM) calculations on peroxidase model systems that the proton shared between glutamic acid and the proximal histidine is located on histidine in most of the studied states [76]. However, our test calculations on small model systems of C-type oxidases suggest that the stabilization of the $\mathbf{I_P}$ intermediate in the cbb_3 models is not very sensitive to the exact location of the proton; when the proton is constrained to the histidine the energy of the $\mathbf{I_P}$ intermediate increases only by 2 kcal/mol.

The cross-linked tyrosine in the cbb_3-model has somewhat perturbed properties relative to the aa_3-model, due to its different orientation and the missing hydroxyethyl farnesyl side chain of heme b_3. The Tyr has a more negative charge in the cbb_3-models than in the aa_3-models, which also polarizes the bridging water molecule more positive in the former system (Table 4). Electrostatically, this leads to a relative destabilization of the peroxy intermediate in cbb_3 (Table 3), which is compensated by the effects discussed above (section 3.3). The different orientation of the Tyr in the two model systems ($\mathbf{A_L}$ and $\mathbf{C_L}$) requires different orientation of the oxygenous ligand relative to the heme system, resulting in different Cu—O^d non-bonded distances in the **A** and $\mathbf{I_P}$ states (Table 2, Fig. 1). However, this distance is similar for both model systems in the $\mathbf{P_M}$ state, where the hydroxyl (—OH^-) is bound to Cu_B and hydrogen-bonded to the oxygen atom attached to the heme iron (Fig. 1c and f, Table 2). The hydrogen-bonding distance from Tyr to the oxygenous iron ligand via the bridging water molecule is 0.3 Å shorter in the cbb_3 enzyme (sum over the two H-bonds), indicating that the barrier for proton transfer may be lower than in the aa_3 enzyme. Due to the distinctively low redox potential of heme b_3 [22] it was suggested that the cross-linked Tyr might only work as a proton donor instead of donating its electron as in the aa_3 enzymes [28]. Providing a more efficient proton transfer pathway from tyrosine to dioxygen via the water molecule in the cbb_3 enzyme might thus also favor the oxygen scission reaction.

4. Conclusions

DFT calculations on the active site of aa_3- and cbb_3-type oxidases suggest that structural features of both the proximal and distal heme surroundings are responsible for the much higher apparent dioxygen affinity shown by the latter enzymes. The proximal histidine is hydrogen-bonded to a glutamate, which partially deprotonates the histidine at least upon oxidation of the heme, and stabilizes a higher oxidation state of the heme iron. The cross-linked tyrosine on the distal side of the heme has a different orientation and H-bonding partners, which might lead to a faster proton transfer reaction to the oxygenous ligand in the cbb_3 enzymes. Stabilization of the peroxy intermediate provides an efficient kinetic trap for the dioxygen binding, increasing the apparent affinity for dioxygen, a property important for organisms living in microaerobic conditions.

Supplementary materials related to this article can be found online at doi:10.1016/j.bbabio.2011.02.002.

Acknowledgments

V.S. is supported by the Viikki Graduate School in Molecular Biosciences. V.R.I.K. acknowledges the European Molecular Biology Organization (EMBO) for a Long-Term fellowship and the Intramural Research Program of the National Institutes of Health, National Institute of Diabetes and Digestive and Kidney Diseases for support. The work was supported by Sigrid Jusélius Foundation, Biocentrum Helsinki and the Academy of Finland. Center for Scientific Computing (CSC), Finland is acknowledged for providing computing support.

References

[1] S. Ferguson-Miller, G.T. Babcock, Heme copper terminal oxidases, Chem. Rev. 96 (1996) 2889–2908.
[2] J.P. Hosler, S. Ferguson-Miller, D.A. Mills, Energy transduction: proton transfer through the respiratory complexes, Ann. Rev. Biochem. 75 (2006) 165–187.
[3] V.R.I. Kaila, M.I. Verkhovsky, M. Wikström, Proton-coupled electron transfer in cytochrome oxidase, Chem. Rev. 110 (2010) 7062–7081.
[4] A.A. Konstantinov, S. Siletsky, D. Mitchell, A. Kaulen, R.B. Gennis, The roles of two proton input channels in cytochrome *c* oxidase from *Rhodobacter sphaeroides* probed by the effects of site-directed mutations on time-resolved electrogenic intraprotein proton transfer, Proc. Natl. Acad. Sci. USA 94 (1997) 9085–9090.
[5] R.B. Gennis, Coupled proton and electron transfer reactions in cytochrome oxidase, Front. Biosci. 9 (2004) 581–591.
[6] P. Brzezinski, Redox-driven membrane-bound proton pumps, Trends Biochem. Sci. 29 (2004) 380–387.
[7] M. Wikström, M.I. Verkhovsky, Mechanism and energetics of proton translocation by the respiratory heme-copper oxidases, Biochim. Biophys. Acta. 1767 (2007) 1200–1214.
[8] V.R.I. Kaila, M.I. Verkhovsky, G. Hummer, M. Wikström, Mechanism and energetics by which glutamic acid 242 prevents leaks in cytochrome *c* oxidase, Biochim. Biophys. Acta. 1787 (2009) 1205–1214.
[9] M. Wikström, C. Ribacka, M. Molin, L. Laakkonen, M.I. Verkhovsky, A. Puustinen, Gating of proton and water transfer in the respiratory enzyme cytochrome *c* oxidase, Proc. Natl. Acad. Sci. USA 102 (2005) 10478–10481.
[10] J. Hendriks, U. Gohlke, M. Saraste, From NO to OO: nitric oxide and dioxygen in bacterial respiration, J. Bioener. Biomemb. 30 (1998) 15–24.
[11] M.M. Pereira, M. Santana, M. Teixeira, A novel scenario for the evolution of haem-copper oxygen reductases, Biochim. Biophys. Acta. 1505 (2001) 185–208.
[12] V. Sharma, A. Puustinen, M. Wikström, L. Laakkonen, Sequence analysis of the cbb_3 oxidases and an atomic model for the *Rhodobacter sphaeroides* enzyme, Biochemistry 45 (2006) 5754–5765.
[13] J. Hemp, R.B. Gennis, Diversity of the heme-copper superfamily in archaea: insights from genomics and structural modeling, Results Probl. Cell Differ. 45 (2008) 1–31.
[14] B. Chance, J.S. Leigh Jr., Oxygen intermediates and mixed valence states of cytochrome oxidase: infrared absorption difference spectra of compounds A, B, and C of cytochrome oxidase and oxygen, Proc. Natl. Acad. Sci. USA 74 (1977) 4777–4780.
[15] D.A. Proshlyakov, M.A. Pressier, C. DeMaso, J.F. Leykam, D.L. DeWitt, G.T. Babcock, Oxygen activation and reduction in respiration: involvement of redox-active tyrosine 244, Science 290 (2000) 1588–1591.
[16] J.E. Morgan, M.I. Verkhovsky, G. Palmer, M. Wikström, Role of the P_R intermediate in the reaction of cytochrome *c* oxidase with O_2, Biochemsitry 40 (2001) 6882–6892.
[17] T.M. Makris, I. Denisov, I. Schlichting, S.G. Sligar, in: Paul R. Ortiz de Monetellano (Ed.), Cytochrome P450, structure mechanism and biochemistry, Third Edition, Kluwer Academic/Plenum Publilshers, New York, 2005, pp. 149–170.
[18] S. Buschmann, E. Warkentin, H. Xie, J.D. Langer, U. Ermler, H. Michel, The structure of cbb_3 cytochrome oxidase provides insights into proton pumping, Science 329 (2010) 327–330.
[19] R.S. Pitcher, N.J. Watmough, The bacterial cytochrome cbb_3 oxidases, Biochim. Biophys. Acta. 1655 (2004) 388–399.
[20] R.S. Pitcher, T. Brittain, N.J. Watmough, Complex interactions of carbon monoxide with reduced cytochrome cbb_3 oxidase from *Pseudomonas stutzeri*, Biochemistry 42 (2003) 11263–11271.
[21] S. Stavrakis, K. Koutsoupakis, E. Pinakoulaki, A. Urbani, M. Saraste, C. Varotsis, Decay of the transient Cu_B-CO complex is accompanied by formation of the heme Fe–CO complex of cytochrome cbb_3-CO at ambient temperature: evidence from time-resolved Fourier Transform Infrared spectroscopy, J. Am. Chem. Soc. 124 (2002) 3814–3815.
[22] V. Rauhamäki, D.A. Bloch, M.I. Verkhovsky, M. Wikström, Active site of cytochrome cbb_3, J. Biol. Chem. 284 (2009) 11301–11308.
[23] J. Hemp, C. Christian, B. Barquera, R.B. Gennis, T.J. Martinez, Helix switching of a key active-site residue in the cytochrome cbb_3 oxidases, Biochemistry 44 (2005) 10766–10775.
[24] J. Hemp, H. Han, J.H. Roh, S. Kaplan, T.J. Martinez, R.B. Gennis, Comparative genomics and site-directed mutagenesis support the existence of only one input channel for protons in the C-family (cbb_3 oxidase) of heme-copper oxygen reductases, Biochemistry 46 (2007) 9963–9972.
[25] V. Rauhamäki, M. Baumann, R. Soliymani, A. Puustinen, M. Wikström, Identification of a histidine-tyrosine cross-link in the active site of the cbb_3-type cytochrome *c* oxidase from *Rhodobacter sphaeroides*, Proc. Natl. Acad. Sci. USA 103 (2006) 16135–16140.
[26] J. Hemp, D.E. Robinson, K.B. Ganesan, T.J. Martinez, N.L. Kelleher, R.B. Gennis, Evolutionary migration of a post-translationally modified active-site residue in the proton-pumping heme-copper oxygen reductases, Biochemistry 45 (2006) 15405–15410.
[27] V. Sharma, M. Wikström, L. Laakkonen, Modeling the active-site structure of the cbb_3-type oxidase from *Rhodobacter sphaeroides*, Biochemistry 47 (2008) 4221–4227.
[28] V. Sharma, M. Wikström, V.R.I. Kaila, Redox-coupled proton transfer in the active site of cytochrome cbb_3, Biochim. Biophys. Acta. 1797 (2010) 1512–1520.
[29] T. Tsukihara, K. Shimokata, Y. Katayama, H. Shimada, K. Muramoto, H. Aoyama, M. Mochizuki, K. Shinzawa-Itoh, E. Yamashita, M. Yao, Y. Ishimura, S. Yoshikawa, The low-spin heme of cytochrome *c* oxidase as the driving element of the proton-pumping process, Proc. Natl. Acad. Sci. USA 100 (2003) 15304–15309.
[30] H. Chang, J. Hemp, Y. Chen, J.A. Fee, R.B. Gennis, The cytochrome ba_3 oxygen reductase from *Thermus thermophilus* uses a single input channel for proton delivery to the active site and for proton pumping, Proc. Natl. Acad. Sci. USA 106 (2009) 16169–16173.

[31] M.I. Verkhovsky, J.E. Morgan, M. Wikström, Oxygen binding and activation: early steps in the reaction of oxygen with cytochrome c oxidase, Biochemistry 33 (1994) 3079–3086.
[32] P.E.M. Siegbahn, M.R.A. Blomberg, Proton pumping mechanism in cytochrome *c* oxidase, J. Phys. Chem. 112 (2008) 12772–12780.
[33] M.R.A. Blomberg, P.E.M. Siegbahn, Quantum chemistry applied to the mechanisms of transition metal containing enzymes—cytochrome *c* oxidase a particularly challenging case, J. Comp. Chem. 27 (2006) 1373–1384.
[34] M. Kaukonen, Calculated reaction cycle of cytochrome *c* oxidase, J. Phys. Chem. B 111 (2007) 12543–12550.
[35] P.E.M. Siegbahn, M.R.A. Blomberg, M.L. Blomberg, A theoretical study of the energetics of proton pumping and oxygen reduction in cytochrome oxidase, J. Phys. Chem. B 107 (2003) 10946–10955.
[36] Y. Yoshioka, H. Kawai, K. Yamaguchi, Theoretical study of role of H_2O molecule on initial stage of reduction of O_2 molecule in active site of cytochrome *c* oxidase, Chem. Phys. Lett. 374 (2003) 45–52.
[37] A.V. Pisliakov, P.K. Sharma, Z.T. Chu, M. Haranczyk, A. Warshel, Electrostatic basis for the unidirectionality of the primary proton transfer in cytochrome *c* oxidase, Proc. Natl. Acad. Sci. USA 105 (2008) 7726–7731.
[38] Y. Yoshioka, H. Satoh, M. Mitani, Theoretical study on electronic structures of FeOO, FeOOH, FeO(H_2O), and FeO in hemes: as intermediate models of dioxygen reduction in cytochrome *c* oxidase, J. Inorg. Biochem. 101 (2007) 1410–1427.
[39] V.R.I. Kaila, M.I. Verkhovsky, G. Hummer, M. Wikström, Glutamic acid 242 is a valve in the proton pump of cytochrome *c* oxidase, Proc. Natl. Acad. Sci. USA 105 (2008) 6255–6259.
[40] V.R.I. Kaila, V. Sharma, M. Wikström, The identity of the transient proton loading site of the proton-pumping mechanism of cytochrome *c* oxidase, Biochim. Biophys. Acta. 1807 (2011) 80–84.
[41] V. R. I. Kaila, M. P. Johansson, D. Sundholm, M. Wikström, Inter-heme electron tunneling in cytochrome *c* oxidase, Proc. Natl. Acad. Sci. USA. In press.
[42] E. Fadda, C.H. Yu, R. Pomès, Electrostatic control of proton pumping in cytochrome *c* oxidase, Biochim. Biophys. Acta. 1777 (2008) 277–284.
[43] Y. Song, E. Michonova-Alexova, M.R. Gunner, Calculated proton uptake on anaerobic reduction of cytochrome *c* oxidase: is the reaction electroneutral? Biochemistry 45 (2006) 7959–7975.
[44] M.R.A. Blomberg, P.E.M. Siegbahn, G.T. Babcock, M. Wikström, Modeling cytochrome oxidase—a quantum chemical study of the O—O bond cleavage mechanism, J. Am. Chem. Soc. 122 (2000) 12848–12858.
[45] M.R. Blomberg, P.E. Siegbahn, M. Wikström, Metal-bridging mechanism for O—O bond cleavage in cytochrome *c* oxidase, Inorg. Chem. 42 (2003) 5231–5243.
[46] M.R. Blomberg, P.E. Siegbahn, G.T. Babcock, M. Wikström, O—O bond splitting mechanism in cytochrome oxidase, J. Inorg. Biochem. 80 (2000) 261–269.
[47] J.A. Fee, D.A. Case, L. Noodleman, Toward a mechanism of proton pumping by the B-type cytochrome *c* oxidases: application of density functional theory to cytochrome ba_3 of *Thermus thermophilus*, J. Am. Chem. Soc. 130 (2008) 15002–15021.
[48] A. Harrenga, H. Michel, The cytochrome *c* oxidase from *Paracoccus denitrificans* does not change the metal center ligation upon reduction, J. Biol. Chem. 274 (1999) 33296–33299.
[49] A.D. Becke, Density-functional exchange-energy approximation with correct asymptotic behaviour, Phys. Rev. A 38 (1988) 3098–3100.
[50] J.P. Perdew, Density-functional approximation for the correlation energy of the inhomogeneous electron gas, Phys. Rev. B 33 (1986) 8822–8824.
[51] A. Schäfer, H. Horn, R. Ahlrichs, Fully optimized contracted Gaussian basis sets for atoms Li to Kr, J. Chem. Phys. 97 (1992) 2571–2577.
[52] A. Schäfer, C. Huber, R. Ahlrichs, Fully optimized contracted Gaussian basis sets of triple zeta valence quality for atoms Li to Kr, J. Chem. Phys. 100 (1994) 5829–5835.
[53] M. Sierka, A. Hogekamp, R. Ahlrichs, Fast evaluation of the coulomb potential for electron densities using multipole accelerated resolution of identity approximation, J. Chem. Phys. 118 (2003) 9136–9148.
[54] C. Lee, W. Yang, R.G. Parr, Development of the Colle–Salvetti correlation-energy formula into a functional of the electron density, Phys. Rev. B Condens. Matter 53 (1988) 785–789.
[55] A. Klamt, G. Schuurmann, COSMO: a new approach to dielectric screening in solvents with explicit expressions for the screening energy and its gradient, J. Chem. Soc. Perkin Trans. 2 (1993) 799–805.
[56] R. Ahlrichs, M. Bär, M. Häser, H. Horn, C. Kölmel, Electronic structure calculations on workstation computers: the program system turbomole, Chem. Phys. Lett. 162 (1989) 165–169.
[57] W. Humphrey, A. Dalke, K. Schulten, VMD—visual molecular dynamics, J. Mol. Graph. 14 (1996) 33–38.
[58] M.R. Blomberg, P.E. Siegbahn, Quantum chemistry as a tool in bioenergetics, Biochim. Biophys. Acta. 1797 (2010) 129–142.
[59] P.E. Siegbahn, M.R. Blomberg, Quantum chemical studies of proton-coupled electron transfer in metalloenzymes, Chem. Rev. 110 (2010) 7040–7061.
[60] B. Chance, C. Saronio, J.S. Leigh Jr., Functional intermediates in the reaction of membrane-bound cytochrome oxidase with oxygen, J. Biol. Chem. 250 (1975) 9226–9337.
[61] M.I. Verkhovsky, J.E. Morgan, A. Puustinen, M. Wikström, Kinetic trapping of oxygen in cell respiration, Nature 380 (1996) 268–270.
[62] L.M. Blomberg, M.R.A. Blomberg, P.E.M. Siegbahn, A theoretical study on the binding of O2, NO and CO to heme proteins, J. Inorg. Biochem. 99 (2005) 949–958.
[63] L. Noodleman, D.A. Case, Density-functional theory of spin polarization and spin coupling in iron–sulfur clusters, Adv. Inorg. Chem. 38 (1992) 423–470.
[64] S. Grimme, Accurate description of Van der waals complexes by density functional theory including empirical corrections, J. Comp. Chem. 25 (2004) 1463–1473.
[65] S. Grimme, Semiempirical ggc-type density functional constructed with a long-range dispersion contribution, J. Comp. Chem. 27 (2006) 1787–1799.
[66] I. Belevich, V.B. Borisov, M.I. Verkhovsky, Discovery of the true peroxy intermediate in the catalytic cycle of terminal oxidases by real-time measurements, J. Biol. Chem. 282 (2007) 28514–28519.
[67] I. Belevich, V.B. Borisov, D.A. Bloch, A.A. Konstantinov, M.I. Verkhovsky, Cytochrome *bd* from *Azotobacter vinelandii*: evidence for high-affinity oxygen binding, Biochemsitry 46 (2007) 11177–11184.
[68] H. Aoyama, K. Muramoto, K. Shinzawa-Itoh, K. Hirata, E. Yamashita, T. Tsukihara, T. Ogura, S. Yoshikawa, A peroxide bridge between Fe and Cu ions in the O_2 reduction site of fully oxidized cytochrome *c* oxidase could suppress the proton pump, Proc. Natl. Acad. Sci. USA 106 (2009) 2165–2169.
[69] J. Koepke, E. Olkhova, H. Angerer, H. Muller, G. Peng, H. Michel, High resolution crystal structure of *Paracoccus denitrificans* cytochrome *c* oxidase: new insights into the active site and proton transfer pathways, Biochim. Biophys. Acta. 1787 (2009) 635–645.
[70] V. R. I. Kaila, E. Oksanen, A. Goldman, D. A. Bloch, M. I. Verkhovsky, D. Sundholm, M. Wikström, A combined quantum chemical and crystallographic study on the oxidized binuclear center of cytochrome *c* oxidase, Biochim. Biophys. Acta. In press
[71] U.C. Singh, P.A. Kollman, An approach to computing electrostatic charges for molecules, J. Comp. Chem. 5 (1984) 129–145.
[72] D.B. Goodin, D.E. McRee, The Asp–His–iron triad of cytochrome c peroxidase controls the reduction potential electronic structure, and coupling of the tryptophan free radical to the heme, Biochemistry 32 (1993) 3313–3324.
[73] J.H. Dawson, M. Sono, Cytochrome P450 and chloroperoxidase: thiolate ligated heme enzymes. Spectroscopic determination of their active site structures and mechanistic implications of thiolate ligation, Chem. Rev. 87 (1987) 1255–1276.
[74] M. Sono, M.P. Roach, E.D. Coulter, J.H. Dawson, Heme containing oxygenases, Chem. Rev. 96 (1996) 2841–2888.
[75] F. Olgiaro, S.P. de Visser, S. Shaik, The 'push' effect of the thiolate ligand in cytochrome P450: a theoretical gauging, J. Inorg. Biochem. 91 (2002) 554–567.
[76] J. Heimdal, P. Rydberg, U. Ryde, Protonation of the proximal histidine ligand in haem peroxidases, J. Phys. Chem. B 112 (2008) 2501–2510.
[77] K.P. Jensen, U. Ryde, Importance of proximal hydrogen bonds in haem proteins, Mol. Phys. 101 (2003) 2003–2018.